# Dry lithiation studies of nanostructured sputter deposited molybdenum oxide thin films

A. TAJ, P. V. ASHRIT
Thin Films and Photonics Research Group (GCMP), Department of Physics and Astronomy, Université de Moncton, Moncton, New Brunswick, Canada E1A 3E9
E-mail: ashritp@umoncton.ca

Transition metal oxides (TMO) with their multiple oxidation states present a wide range of interesting properties based on electron transition between these states [1]. Amongst these are the chromogenic properties, wherein one can induce a reversible optical property change under the influence of various stimuli such as an electric field (electrochromic, EC), light impingement (photochrome, PC), heat (thermochrome, TC), and gas exposure (gasochromic, GC) [2]. A vast amount of research work is dedicated to the study of the electrochromic (EC) effect in various TMOs [3]. Most of the research attention has been paid to the study of tungsten trioxide (WO_3), which has been found to be an excellent candidate exhibiting an efficient reflectance and absorption modulation depending on the structure and phase of the film. Much of the current work is directed toward improving the coloration efficiency of the TMO thin films. It has been found in these WO_3 [4] and other films [5] that the nanostructuring of the films renders them highly electrochromically efficient. The molybdenum oxide (MoO_3) thin films, on the other hand, have received a comparatively insignificant amount of research attention, despite their EC performance paralleling that of WO_3 films. Molybdenum oxide (MoO_3) thin films which exhibit a cathodic coloration under lithium ion/electron double injection, have a fairly high mixed ion-electron conductivity. The optical change that occurs in these films can be represented as follows [6]:

$$MoO_3(\text{clear}) + x\text{Li}^+ + x\text{e}^- \leftrightarrow \text{Li}_x MoO_3(\text{colored})$$
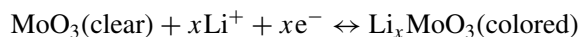
where, under the double insertion of x number of lithium ions and electrons (e^-) the clear film of MoO_3 is transformed reversibly into dark blue colored bronze, $\text{Li}_x MoO_3$. Not much work has been carried out to examine the effect of micro or nanostructuring of the MoO_3 thin films [7] on its electrochromic performance. In this work the electrochromic performance of RF sputtered nanostructured MoO_3 films has been studied by our laboratory developed dry lithiation method. Here, instead of the separate insertion of lithium ions and electrons as indicated earlier, neutral atoms of lithium are injected into the film under study [8]. This study of dry lithiation has been applied for the first time on MoO_3 films. The structural evolution and electrochromic coloration with lithium insertion have been studied.

The molybdenum oxide (MoO_3) thin films used in this study were prepared on clean glass substrates by r.f. magnetron sputtering using a molybdenum oxide target (purity 99.99%). Three films with varying thickness studied here were prepared at a pressure of 2.5×10^{-3} Torr, and using a water-cooled cold finger in the presence of Ar–O_2 mixture at an Ar to O_2 ratio of 4 to 1. The film thickness and the optical constants were determined from a laboratory built reflection/transmission
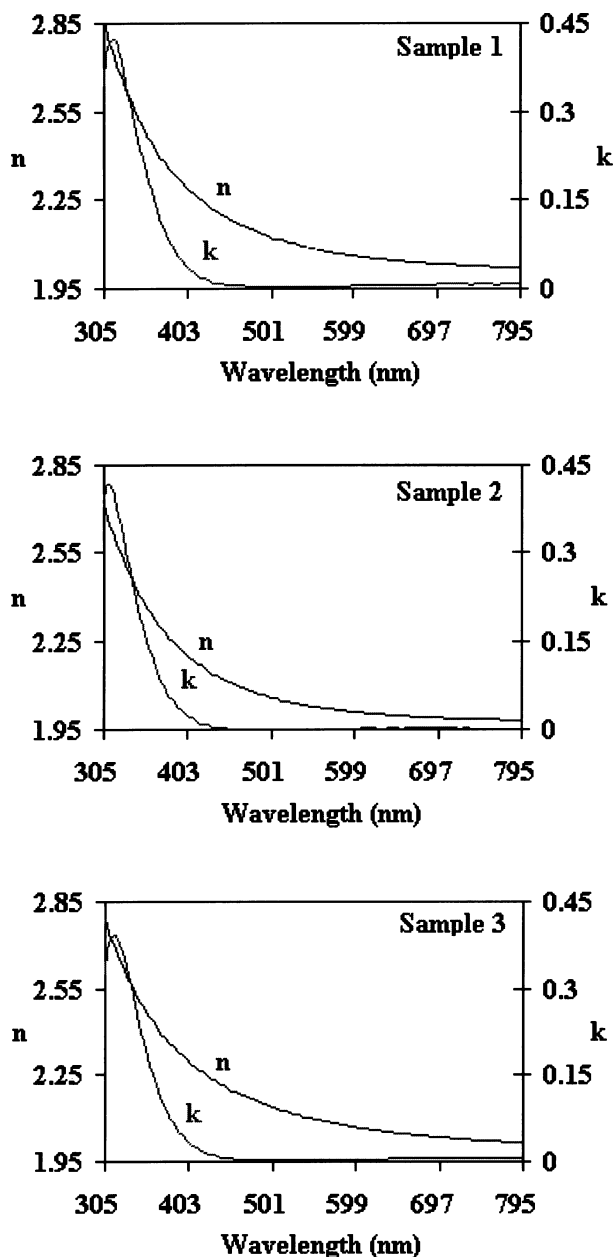

Figure 1 Optical constants (n, k) for the three samples as determined by the reflection/transmission ellipsometry.

3541

ellipsometer and a thin film analysis software. The three samples with a thickness of 210.6 nm (Sample 1), 162.5 nm (Sample 2), and 252.6 nm (Sample 3) were deposited at the rate of approximately 0.2 nm/s. Dry lithiation was achieved by exposing the samples under vacuum to neutral lithium atoms emanating from lithium niobate ($LiNbO_3$) heat-treated from a tungsten filament. The degree of such lithiation was measured by noting the change in the quartz crystal thickness (effective mass) and calibrated against the electrochemical insertion to arrive at the actual charge inserted [8]. A

Digital Instruments Nanoscope (Dimension 3100) was used to study the film structure.

In Fig. 1 are given the optical constant (n, k) values for the three samples as determined by the reflection/transmission ellipsometry. The nature of n and k variation in all the three samples is quite similar, although Sample 2 exhibits a slightly inferior n value compared to the other two samples. Taking the reference of the 632-nm wavelength, the three samples exhibit an n value of between 2 and 2.05 compared to the most commonly reported bulk value of 2.2 at this
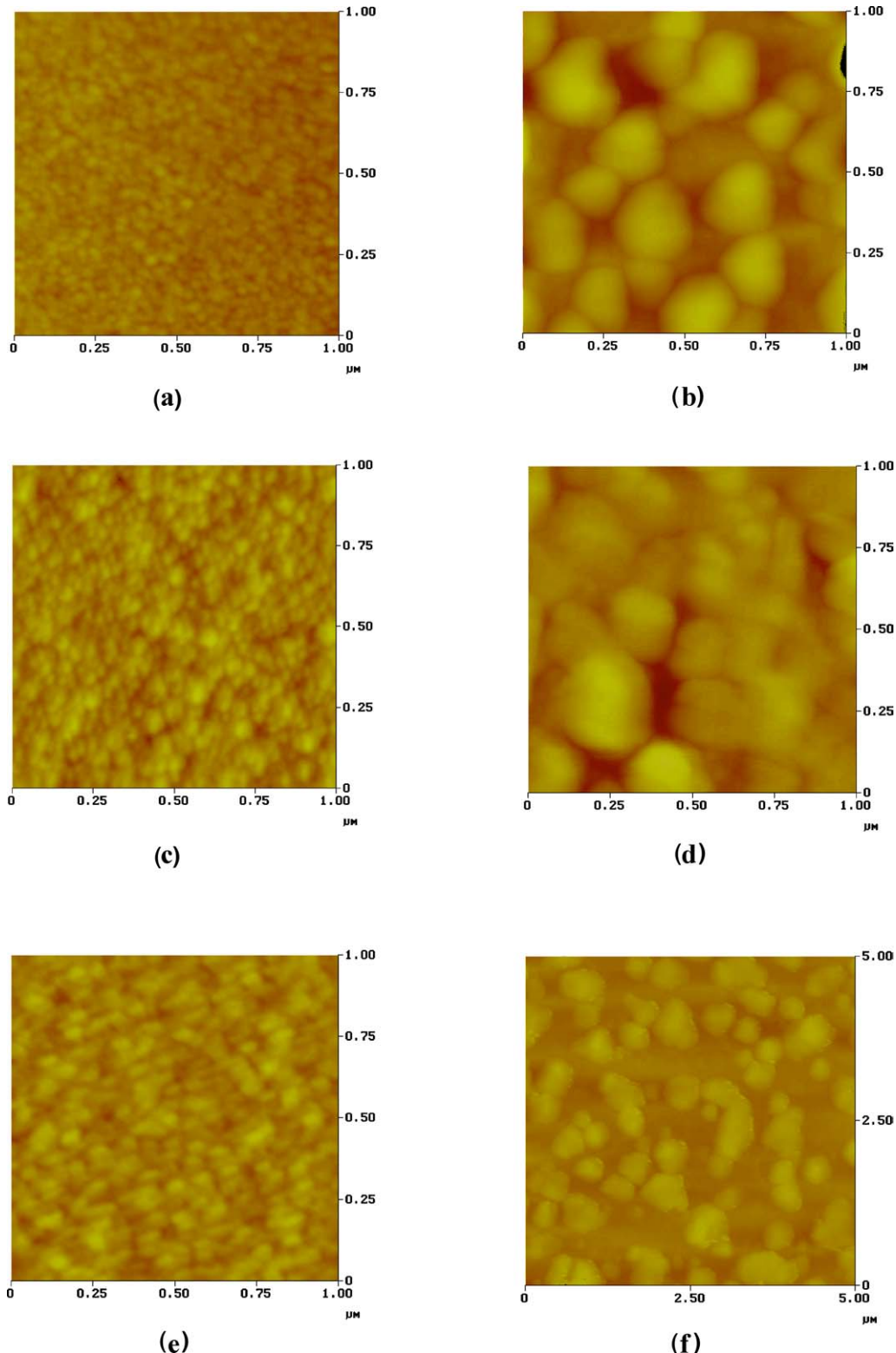

Figure 2 Atomic force micrographs of Sample 1 with the insertion of: (a) 0 nm, (b) 2.5 nm, (c) 5 nm, (d) 10 nm, (e) 15 nm and (f) 20 nm of lithium.

wavelength. Hence, the film density can be expected to be quite close to that of the bulk in these samples.

The atomic force micrographs (AFM) indicated a fairly comparable nanostructure in the three as-deposited samples studied (see, for example, Fig. 2a). The average grain size of the samples was found to vary between 48 and 60 nm. The AFM images shown for Sample 1 (Fig. 2) with the intercalation of lithium clearly indicate the evolution of the film nanostructure. The average grain size of the 48 nm found in Sample 1 in the as-deposited state seems to inflate gradually to 50 nm (2.5 nm Li), 85 nm (5 nm Li), 180 nm (10 nm Li). Further lithium insertion beyond 10 nm, as can be seen in this figure, seems to distort the surface structure. This is seen for the case of 15 and 20 nm. This distortion seems to precipitate large particles with an average size of 420 nm on the surface, as seen for the insertion of 20 nm of lithium. An effective mass of 10 nm corresponds to the insertion of 6.25 mC/cm^2 of lithium charge insertion. Hence, it seems at least at the surface level that the lithium insertion saturates between 10 and 15 nm of effective mass thickness.

The normal state optical properties and the optical changes occurring in the as-deposited film with the lithium insertion are shown in Fig. 3 in the form of transmission (T) spectra. All the three samples exhibit a very high degree of transmission throughout the spectral region studied. With increasing lithium insertion, a very effective absorption band spanning the higher visible and lower NIR region develops. As can be seen from this figure, bulk of the optical modulation is concentrated in the wavelengths region between 300 to 1400 nm in all the three samples. In Sample 1, which exhibits the most efficient coloration, the optical modulation increases gradually with increasing quantity of lithium and seems to approach saturation beyond the insertion of 15 nm. This is to some extent consistent with the AFM film surface observations. The reflection spectra (not shown here) do not seem to change significantly except for the surface effects and the suppression of the interference in the visible wavelengths due to increasing absorption. However, there is a large variation in terms of the nature of this optical modulation between the three samples studied. In Sample 2, the optical modulation peak is found to move slightly to lower wavelengths with lithium insertion. The saturation here is achieved much earlier, i.e., with the insertion of 10-nm mass thickness of lithium, as compared to Sample 1. Lithium insertion beyond this point seems to change the coloration only in the mid-visible region. The optical modulation in this region saturates clearly around 15 nm. Sample 3 exhibits the most dissimilar optical behavior under lithium insertion. With increasing lithium insertion the modulation peak seems to move toward higher wavelengths and the optical change saturates for 10-nm lithium insertion. With further lithium insertion, no further changes are seen anywhere in the spectral region studied.

In order to get a better idea of the optical modulation behavior, the coloration efficiency (CE), which is defined [3] as the ratio between optical density change ($\Delta OD = \log(T_{uncolored}/T_{colored})$) and the charge inserted
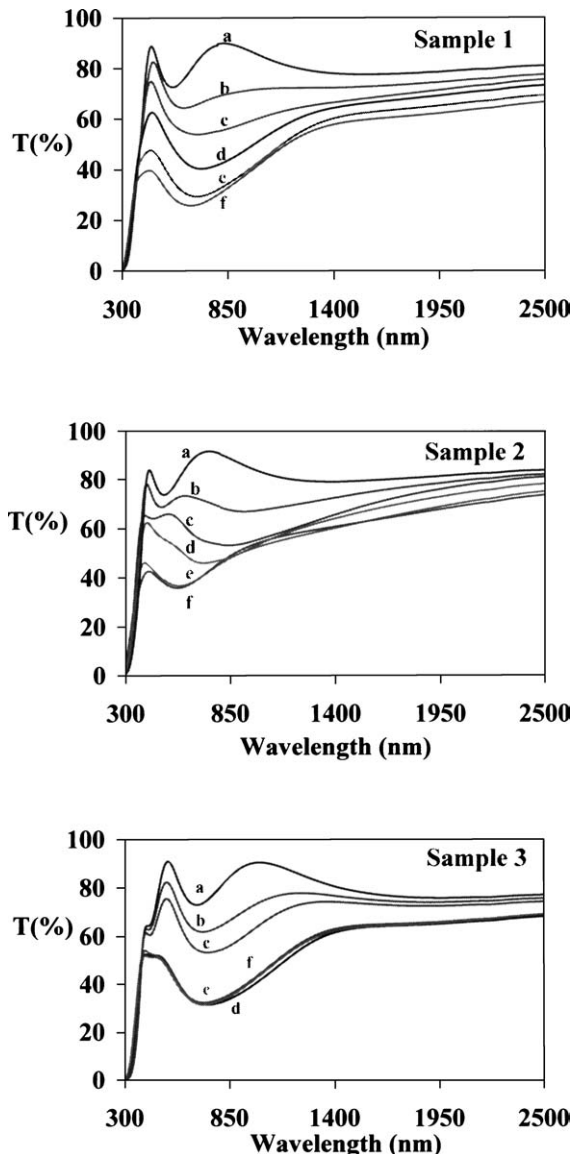

Figure 3 Transmission spectra of the various MoO$_3$ thin films with the lithium insertion of: (a) 0 nm, (b) 2.5 nm, (c) 5 nm, (d) 10 nm, (e) 15 nm and (f) 20 nm.

(Q), is given for the three samples for the charge insertion of 12.5 cm^2/C i.e., 20 nm of effective mass thickness. As can be seen from Fig. 4, the coloration efficiency is the most effective for Sample 1, reaching a peak value of around 40 cm^2/C, at the wavelength of about 750 nm. Sample 2 exhibits a similar spectral nature of modulation but with a much-reduced efficiency. The peak CE value that occurs at a wavelength of 625 nm is found to be around 30 mC/cm^2. On the other hand, in Sample 3 it is seen that the CE peak moves to higher wavelengths with a peak value of around 30 cm^2/C centered around the wavelength of 850 nm. Hence, it is clear that Sample 1 exhibits the most efficient coloration both in terms of its effectiveness and the wavelengths span over which this occurs.

Dry lithiation, which is a convenient method to characterize the electrochromic behavior, has been employed for the first time to intercalate the MoO$_3$ thin films and to follow the structural and optical evolution of these films. Experimental work concerning the
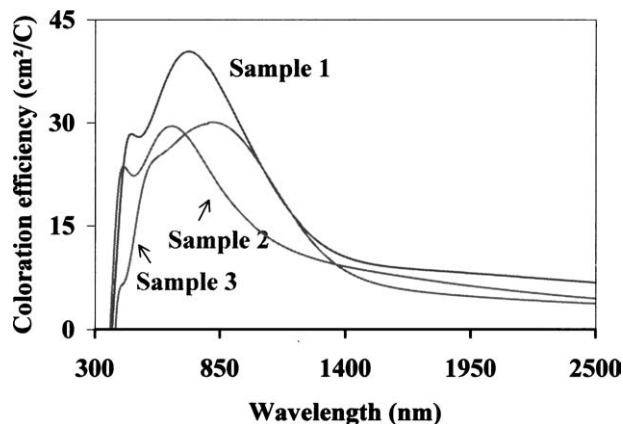
Figure 4 Coloration efficiency (CE) of the various MoO_3 samples calculated for the insertion of 20-nm lithium.

chromogenic property dependence on the film thickness of sputter deposited MoO_3 thin films has been carried out. The nanostructure of the as-deposited film and the evolution of it as a function of lithium insertion have been studied with three different film thicknesses. From the study of the optical changes it has been found that there is an optimum thickness in sputter deposited MoO_3 films, which gives a broadband and intense optical modulation. It has also been found that the AFM structural study can be used to get an idea of the reversible regime of lithium insertion and EC coloration.

More work on these films is currently being carried out to examine these implications by detailed ellipsometric and electrochemical methods.

References
1. M. IMADA, A. FUJIMORI and Y. TOKURA, *Rev. Phys.* **70** (1998) 1039.
2. C. M. LAMPERT and C. G. GRANQVIST, "Large Area Chromogenics: Materials and Devices for Transmittance Control," Vol. IS4 (SPIE Institute Series, Bellingham, 1990).
3. C. G. GRANQVIST, "Handbook of Inorganic Electrochromic Materials," 2nd ed. (Elsevier, 2002).
4. P. V. ASHRIT, *Thin Solid Films* **385** (2001) 81.
5. A. HAGFELDT, N. VIACHOPOULOS and M. GRATZEL, *J. Electrochem. Soc.* **141** (1994) L82.
6. BRIAN W. FAUGHNAN, RICHARD S. CRANDALL and PHILIP M. HEYMAN, *RCA Review* **36** (1975) 177.
7. Z. HUSSAIN, *J. Mater. Res.* **16** (2001) 2695.
8. P. V. ASHRIT, G. BADER, F. E. GIROUARD and VO-VAN TRUONG, *SPIE* **1401** (1990) 120.